Plant Cell Rep (2009) 28:469–480
DOI 10.1007/s00299-008-0651-5

GENETICS AND GENOMICS

Highly efficient gene silencing using perfect complementary artificial miRNA targeting *AP1* or heteromeric artificial miRNA targeting *AP1* and *CAL* genes

Wonkeun Park · Jixian Zhai · Jung-Youn Lee

Received: 1 August 2008 / Revised: 27 October 2008 / Accepted: 17 November 2008 / Published online: 9 December 2008

Abstract Gene silencing is a useful technique for elucidating biological function of genes by knocking down their expression. Recently developed artificial microRNAs (amiRNAs) exploit an endogenous gene silencing mechanism that processes natural miRNA precursors to small silencing RNAs that target transcripts for degradation. Based on natural miRNA structures, amiRNAs are commonly designed such that they have a few mismatching nucleotides with respect to their target sites as well as within mature amiRNA duplexes. In this study, we performed an analysis in which the conventional and modified form of an amiRNA was compared side by side. We showed that the amiRNA containing 5′ mismatch with its amiRNA* and perfect complementarity to its target gene acted as a highly potent gene silencing agent against *AP1*, achieving a desired null mutation effect. In addition, a simultaneous silencing of two independent genes, *AP1* and *CAL1* was tested by employing a multimeric form of amiRNAs. Advantages and potential disadvantages of using amiRNAs with perfect complementarity to the target gene are discussed. The results presented here should be helpful in designing more specific and effective gene silencing agents.

Communicated by D. Somers.

Electronic supplementary material The online version of this article (doi:10.1007/s00299-008-0651-5) contains supplementary material, which is available to authorized users.

W. Park · J. Zhai · J.-Y. Lee (✉)
Department of Plant and Soil Sciences,
Delaware Biotechnology Institute,
University of Delaware, Newark,
DE 19711, USA
e-mail: lee@dbi.udel.edu

Present Address:
W. Park
USDA-ARS, Florence, SC, USA

Introduction

Gene silencing, a powerful reverse genetics tool for knocking down gene expression, is commonly used to elucidate or manipulate biological function of novel, agriculturally important genes. Knock-down or gene silencing in plant systems has been commonly achieved by ectopic expression of double-stranded RNAs (dsRNA) (Wesley et al. 2001), viral vectors (Liu et al. 2002; Lu et al. 2003), or artificial miRNAs (amiRNAs) (Alvarez et al. 2006; Niu et al. 2006; Schwab et al. 2006; Warthmann et al. 2008). These approaches exploit *p*ost-*t*ranscriptional *g*ene *s*ilencing (PTGS) or RNA interference (RNAi) mechanisms, which induce degradation (Baulcombe 2004; Brodersen and Voinnet 2006; Filipowicz et al. 2008) or translational inhibition (Aukerman and Sakai 2003; Brodersen et al. 2008) of the target mRNAs that are complementary to the small silencing RNAs. There are two major types of these RNAs, namely short interfering RNAs (siRNAs) and microRNAs (miRNAs), which are processed from different precursor dsRNAs by specialized RNAses called Dicer. Following the production, sRNAs guide the RNA-induced silencing complex (RISC) to cleave the respective target mRNAs, knocking down the expression level of the gene.

The dsRNA gene silencing technique employs ectopic expression of long double-stranded RNAs derived from inverted repeat-containing hairpin (hp) RNA precursors (Chuang and Meyerowitz 2000; Wesley et al. 2001). Typically, hpRNA constructs are composed of sense and anti-sense sequences derived from respective target genes,

which are flanked by an intron sequence. This method was shown to be highly effective in various plant species (Watson et al. 2005). Virus-induced gene silencing (VIGS) utilizes viral vectors to introduce specific sequences that target endogenous genes in a transient expression manner (Liu et al. 2002; Lu et al. 2003). Recently developed amiRNA-based gene silencing techniques exploit the RNAi mechanism operating for naturally occurring microRNAs (miRNAs) (Alvarez et al. 2006; Niu et al. 2006; Schwab et al. 2006; Warthmann et al. 2008). Endogenous miRNAs are processed from non-coding RNA precursors that form double-stranded hairpin structures. The stem region of the hairpin is processed to ~21-nucleotide (nt)-long mature miRNA duplex. The miRNA strand complementary to its target gene is then recognized by the RISC and guides the complex to degrade the target mRNA (Bartel 2004).

The amiRNAs are designed by employing an endogenous miRNA precursor sequence as structural backbone but replacing the stem-loop forming duplex miRNA region with a specific amiRNA sequence (Ossowski et al. 2008). The 21-base-long mature miRNA region of naturally occurring miRNA precursors is replaced with the duplex sequence of amiRNA designed to specifically target a selected gene(s) of interest and its complementary strand amiRNA*. Expression of amiRNA precursors under the control of a strong, constitutive promoter in transgenic plants leads to an accumulation of mature amiRNAs which guide the RISC to cleave their target genes. This amiRNA-based gene silencing technique is functionally effective in various plant species including *Arabidopsis* (Alvarez et al. 2006; Schwab et al. 2006), tobacco (Alvarez et al. 2006), tomato (Alvarez et al. 2006), and rice (Warthmann et al. 2008). Application of this technique is facilitated by the development of an elegant web-based platform, the Web MicroRNA designer (WMD at http://wmd2.weigelworld.org) which allows automated design of amiRNAs for genes of interest (Ossowski et al. 2008). This tool offers computational incorporation of nucleotide mismatches that mimic the characteristics of endogenous plant miRNAs into the design of candidate 21-base amiRNAs so that they complement imperfectly the target sequences.

We have here investigated whether the effectiveness of an existing amiRNA approach could be improved by simple modifications in amiRNA design in a comparative analysis employing the same complementary target site. In this study, we chose as target genes well-characterized and partially redundant *Arabidopsis* floral organ identity genes, *APETALLA1* (*AP1*) (Mandel et al. 1992; Bowman et al. 1993) and *CAULIFLOWER* (*CAL*) (Bowman et al. 1993; Kempin et al. 1995). We compared the effects on target mRNA degradation and plant phenotype by introducing amiRNAs that perfectly complement the target genes or arrayed as a tandem repeat. The latter approach was also tested by producing a tandem array of heteromeric amiRNAs, which have been previously demonstrated to be functional (Parizotto et al. 2004; Alvarez et al. 2006; Niu et al. 2006).

Methods

Plant and other materials

Wild-type and transgenic *Arabidopsis* (Col-0) were grown in controlled growth chambers at 22–25°C in a long-day regime (18 h light/6 h dark cycle). *Arabidopsis* transformation was performed by dipping the inflorescence in the liquid medium containing transformed agrobacteria and selecting independent T1 transformants based on glufosinate resistance.

All the primers/oligonucleotides used to construct amiRNA precursors and other analyses performed in this study are listed in Supplemental Tables 1 and 2.

Modification of pRS300 plasmid vector and construction of amiRNA precursors

First, *Sal*I and *Not*I sites were sequentially removed from pRS300 by repeated fill-in ligation following restriction enzyme digestion. Next, To replace *Bam*H1 in pRS300 with the *Sal*I site, the plasmid was digested with *Bam*H1 and then ligated with an oligo duplex linker containing the *Sal*I site utilizing T4 DNA Ligase (Fermentas). The linker was produced by annealing the two oligos, pRS300m oligo1 and pRS300m oligo2. The resulting plasmid pRS300m contains *Xho*I and *Sal*I sites for cloning of amiRNAs.

Various amiRNAs were amplified from pRS300m in a two-step overlapping PCR through which the miR-*319a* duplex sequence within the hairpin structure was replaced with specific amiRNA and amiRNA* strands. During this amplification, a new *Bam*HI site was incorporated into the 3′ end of the amiRNA precursor product immediately after the *Sal*I site by employing a reverse primer carrying a *Bam*HI cleavage site at the 3′ end (see Fig. 1b). The amiRNA precursor products were thus engineered to include *Xho*I at the 5′ and *Sal*I/*Bam*HI sites at the 3′ ends, respectively, upon completion of the PCR amplification. The *Xho*I and *Bam*HI sites were then used for a directional cloning of amiRNA precursors into a shuttle vector pdM which contains an expression cassette composed of the *Cucumber mosaic virus* 35S promoter and the OCS terminator. Subsequently, the expression cassette flanking the amiRNA precursor insert was released by *Not*I digestion and subcloned into a binary vector, pMLBart to transform *Arabidopsis*.

Two pairs of primers specific to amiRNA and amiRNA* targeting a gene(s) of interest were basically designed

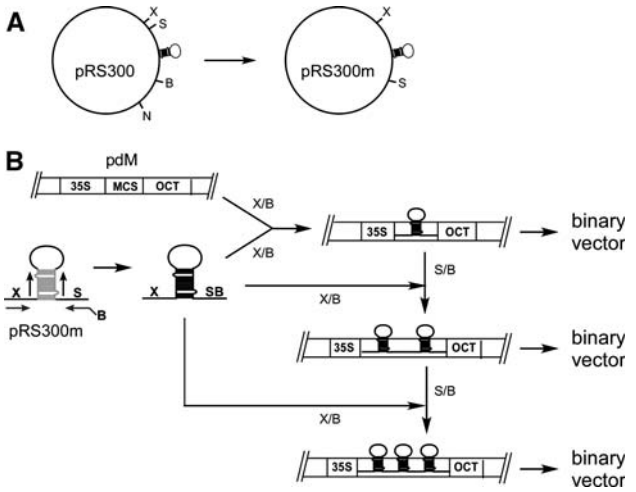

Fig. 1 Construction of amiRNA clones. Restriction enzyme sites are abbreviated to single uppercase letters: X for *Xba*I, S for *Sal*I, B for *Bam*HI, and N for *Not*I. **a** Modification of pRS300 to pRS300 m amiRNA cloning vector plasmid. **b** A schematic diagram illustrating cloning steps for monomeric or multimeric amiRNA clones into an expression vector, pdM and binary vector. *X/B* or *S/B* indicates double digestion steps. Stem region of miR-*319a* template is indicated by *gray bars*

according to the first generation WMD design tool. Primers used for amiR-*ap1*A^{P} were modified manually in order to eliminate a potential targeting of amiR-*ap1*A^{P*} strand and to accommodate the rule of asymmetry between amiRNA and amiRNA* strands (Schwab et al. 2006). To produce three overlapping regions of amiRNA stem-loop sequence, each fragment was individually amplified using *Taq* Polymerase (GeneScript) and 10 ng of pRS300m template by 27 PCR cycles, each consisting of 30 s at 94°C, 45 s at 47–53°C, 40 s at 72°C. The PCR products were column-purified and 1/40 resuspended DNA was used as template in the subsequent overlapping PCR to amplify full-length amiRNA precursors by 25 cycles.

To construct multimeric tandem amiRNA precursors, additional amiRNAs were sequentially added following the cloning of a first amiRNA precursor into pdM. This cloning strategy was previously used to produce multimeric amiRNA hairpins in animal cells (Sun et al. 2006). Construction of tandem repeats of an amiRNA was achieved by repeating the following subcloning steps: first, overlapping PCR products were digested with *Xho*I and *Bam*HI followed by a ligation with the pdM vector digested with *Xho*I and *Bam*HI. Next, the amiRNA insert in the pdM was digested with *Sal*I and *Bam*HI and re-ligated with the amiRNA produced from the overlapping PCR, followed by digestion with *Xho*I and *Bam*HI. pdM plasmid subcloned with single or tandemly repeated amiRNAs was confirmed by DNA sequencing and then digested with *Not*I, which releases the expression cassette including the 35S promoter, OCS terminator, and amiRNA insert(s). This digest fragment was cloned into the *Not*I-digested pMLBart binary vector that confers BASTA resistance in transformed *Arabidopsis*. amiR-*ap1*A*cal*A and amiR-*ck6*A*ck1*A constructs were amplified using pRS300 plasmid as template and Ami-Primer A and B as one of the primer sets. Following the cloning of the first amiRNA precursors into pdM, the second precursors amplified in PCR using ami-primer A2 and B were subcloned into this plasmid using the *Bam*H1 site. DNA clones showing correct orientation of the second amiRNAs were selected by restriction enzyme digestion and used for further subcloning into pMLBart.

RNA blot hybridization

Regular and small RNA blot hybridization was performed as described elsewhere (Park et al. 2002) with minor modifications. Briefly, 0.1 g of each *Arabidopsis* leaf or inflorescence tissue sample (inflorescence or leaf) collected in 1.5 mL microfuge tubes was frozen in liquid nitrogen and ground finely with plastic pestle followed by total RNAs extraction with Trizol (Invitrogen). Total RNA was then precipitated with isopropanol following chloroform extraction. For small RNA Northern, approximately 10 μg of resuspended total RNAs prepared from each sample was fractionated in a 15% denaturing polyacrylamide gel containing 8 M urea followed by a staining of the gel with EtBr and RNA transfer onto a positively charged nylon membrane by electroblotting. RNAs transferred onto a membrane (Zeta probe Blotting membrane, BioRad) was crosslinked by UV in a crosslinker followed by air drying overnight at room temperature. Radioactive probe was synthesized by end-labeling 20 pmole of DNA oligos for 30 min at 37°C in 20 μl reaction containing 1 μl of T4 Polynucleotide Kinase, 2 μl of γ^{32}P-ATP (~6,000 Ci/mmole), and 2 μl of 10× T4 PNK buffer. Small RNA hybridization was performed by incubating an RNA blot in Ultrahyb-oligo hybridization buffer (Ambion) containing a ^{32}P-end-labeled oligonucleotide probes for 16 h at 35–40°C followed by two washes with 2× SSC buffer containing 0.5% SDS at 40°C for 15 min each. Finally, the blot was exposed to X-ray film at −80°C until developed. The sequences of each oligo probe for amiR-*ap1*A and amiR-*ap1*A* are given in Supplemental Table 2. For the evaluation of *AP1* mRNA level in RNA blot hybridization, *AP1*-specific cDNA probe (464 bp) was amplified by PCR using AP1-F2 and AP1-R primers.

Semi-quantitative RT-PCR

Total RNA was extracted from T2 or T3 lines for all of the experiments except T1 lines analyzed in amiR-*ap1*A^{P}*cal*A. Reverse transcription was performed by using MMLV-

reverse transcriptase (NEB), 1 μg total RNA as template, and an oligo-d(T)$_{18}$ primer in a 20 μl reaction volume. Following the reaction for 1 h at 42°C, 1 μl of the reaction mixture was taken for a subsequent PCR reaction (20 μl). *AP1* and *UBIQUITIN* cDNAs were amplified with annealing temperature at 53°C during 28 cycles. *CAL* cDNA was annealed at 50°C and amplified by 30 cycles. Primer pairs used include AP1 F and R for *AP1*, CAL F and R for *CAL* and UBQ F and R for *UBQ*. Twenty microliters of PCR products were fractionated in 0.8–1% agarose gels and quantified by using a densitometric analysis program (AlphaImager) based on replicate RT-PCR reactions with independent plant samples. At least two or more independent plants were sampled from each group and more than two RT-PCR reactions were performed for the quantitative measurement.

Cleavage site mapping by 5′ RACE-PCR

To clone the cleavage products, a RNA ligase-mediated 5′ RACE was performed (FirstChoice RLM-RACE Kit, Ambion) according to the protocol provided by the supplier. Two micrograms total RNA isolated from the influorescence tissue of the transgenic plants were ligated to 5′ RACE adapter followed by RT-PCR using Oligo dT (Invitrogen) and initial PCR using the 5′ RACE and gene-specific outer primers. Nested PCR was then followed by using the 5′ RACE, and gene-specific inner primers. Amplified PCR products were eluted from an agarose gel, cloned into pCR4-TOPO-easy vector (Invitrogen), and sequenced. The sequence specific primers used are included in Supplemental Table 2.

PCR-based methylation detection assay

Detection of methylation of *AP1* genomic DNA was performed as described (Onodera et al. 2005). Approximately 0.5 μg of genomic DNAs isolated by using an extraction buffer (200 mM Tris, pH 7.4, 250 mM NaCl, 25 mM EDTA and 0.5% SDS) and phenol/chloroform mixture from wild-type and amiRNA overexpression lines were subjected to the restriction enzyme *Hae*III (Gibco) treatment for 6 h in 30 μl reaction volume. The reaction was stopped by inactivating the enzyme at 80°C for 20 min, and 1 μl of the digestion products was used as template and AP1 F3 and R as primers for the subsequent PCR amplification by 32 cycles, each composed of 30 s at 94°C, 45 s at 55°C, and 60 s at 72°C for the PCR 1 fragment. Same PCR amplification profile was used to amplify PCR 2 fagment except for changing the annealing temperature to 53°C and the primer set to AP1 F2 and R2.

Results

Construction and functionality test of pRS300m

To facilitate the cloning of monomeric or multimeric amiRNAs, we modified an amiRNA cloning vector plasmid pRS300 which contains miR-*319a* precursor sequence (Schwab et al. 2006) to a new version, pRS300m (Fig. 1a). Primarily, three restriction enzyme sites were altered in pRS300m: *Not*I, *Sal*I and *Bam*HI sites were removed, and one *Sal*I site was reinserted at a new location, i.e., the 3′ end of the multicloning site. The miR-*319a* precursor sequence was not altered in the pRS300m.

Next, functionality of pRS300m containing monomeric or multimeric amiRNAs was tested by performing a control experiment in which a single, double, and triple miR-*319a* were constructed and introduced into *Arabidopsis* (Fig. 1b). Overexpression of miR-*319a* was expected to mimic the *jaw*-D mutant phenotype that was previously shown to be brought about by overexpression of miR-*319a* (Palatnik et al. 2003, 2007). In our study, over 90% T1 plants that express miR-*319a* showed a strong visual phenotype, revealing abnormal leaf morphology similar to the *jaw*-D mutant regardless of the hairpin copy number (data not shown). The severity of morphological phenotypes was so similar among these T1 plants that it was difficult to assess whether multimeric miR-*319a* constructs were more effective than the momomeric form. However, this result allowed us to conclude that the multimeric amiRNAs were functional and at least as effective as the monomeric form in inducing gene silencing.

Efficient gene silencing by multimeric amiRNA

To test whether efficiency or effectiveness of amiRNAs can be increased by simple alterations in amiRNA structure designed by the WMD protocol, we performed a comparative analysis by employing modified amiRNAs with multimeric forms or with perfect complementarity between amiRNA and amiRNA*. We chose a well-characterized floral organ identity gene, *AP1* as an example target. *AP1* has advantages in qualitatively assessing the severity of the gene silencing effect in our study because the extent of morphological phenotypes is well-documented for weak, intermediate, or severe *AP1* mutant alleles. In addition, this gene has been shown to be an effective target for dsRNA- and amiRNA-based gene silencing (Chuang and Meyerowitz 2000; Chen 2004; Alvarez et al. 2006; Schwab et al. 2006). Morphologically, strong *ap1* mutant alleles cause visually distinct phenotypes: formation of leaf-like organs instead of sepals, lack of petals, and development of secondary floral meristems from the base of leaf-like organs

depending on the strength of mutant alleles (Mandel et al. 1992; Bowman et al. 1993; Kempin et al. 1995)

By following the design criteria suggested by the WMD protocol, two best-scored *AP1*-specific target sites were selected to produce corresponding amiRNAs, amiR-*ap1*A and amiR-*ap1*B (Table 1). Precursors for each amiRNA were first constructed in pRS300m and then sequentially subcloned into pdM and pMLBart as illustrated in Fig. 1b to transform *Arabidopsis*. T1 plants that express amiR-*ap1*A or amiR-*ap1*B were analyzed and scored for the extent to which floral morphology was altered (Table 2) as well as for the level of reduction in *AP1* mRNA expression (Fig. 2). Among the T1 plants that express amiR-*ap1*A, ~40% plants showed morphologically obvious phenotypes, half of which exhibiting a strong *ap1* phenotype (Table 2). In contrast, all T1 plants that express amiR-*ap1*B had normal flowers, indicating that this construct was not functional. This conclusion was also confirmed by the RT-PCR analysis, which showed that the amiR-*ap1*B plants had *AP1* expression level comparable to that of wild-type plants.

As the amiR-*ap1*A was functional in down-regulating *AP1* (Fig. 2), we focused on this amiRNA for further studies and made two modifications: one altering amiR-*ap1*A to a trimeric amiR-*ap1*A, keeping its sequence unchanged (amiR-*ap1*AAA), and the other conferring perfect complementarity to the target site by eliminating mismatches in amiR-*ap1*A (amiR-*ap1*A^P) (Table 1). Approximately 80% T1 plants that express amiR-*ap1*AAA showed *ap1* floral mutant phenotypes, and one-third of these plants resembled strong *ap1* mutant alleles (Fig. 2b). To test whether this seemingly more efficient gene silencing was also correlated with a higher level of reduction in *AP1* mRNA expression, we performed RNA blot hybridization and semi-quantitative RT-PCR analyses on the plants exhibiting a similar extent of strong mutant phenotype (Fig. 2c, d). These experiments showed that both amiR-*ap1*A and amiR-*ap1*AAA were effective in down-regulating the target gene *AP1*, and the level of reduction in *AP1* mRNA expression by the two amiRNAs was similar. Densitometric measurement of RT-PCR products showed that *AP1* mRNA expression was decreased by ~60% in amiR-*ap1*A and amiR-*ap1*AAA plants (Fig. 2d), indicating that both forms were similarly effective in *AP1* mRNA degradation. These results suggested that both monomeric amiR-*ap1*A and trimeric amiR-*ap1*AAA were similar in terms of the target gene degradation. It is notable that a higher percentage of amiR-*ap1*AAA T1 plants showed knock-down mutant phenotype. One possibility is that multimeric forms of amiRNA may be less subjected to a positional effect of the T-DNA insertion in transgenic plants and can accumulate over the effective threshold level more consistently than the monomeric form.

Efficient gene silencing by amiRNAs with perfect complementarity to the targets

Next, we examined whether the amiRNA design could be simplified by allowing perfect complementarity between an amiRNA and its target site without compromising its effectiveness. For this test, we modified amiR-*ap1*A to amiR-*ap1*A^P by removing mismatches to *AP1* at nucleotide positions 1 and 20 of the mature amiRNA strand (Table 1). Surprisingly, phenotypical analysis showed that over 95% amiR-*ap1*A^P T1 plants produced *ap1* mutant flowers and

Table 1 Forms and sequences of amiRNAs targeting *AP1* and/or *CAL*

Transgenic line[a]	Form (mismatch)	Target and predicted mature amiRNA sequences			ΔG (kcal/mol)
amiR-*ap1*A	Monomer (1.5)	*AP1* mRNA	770-790	AUCCAGCAUCCUUACAUGCUC	−39.55
				|:||||||||||||||||||	
		amiR-*ap1*A	3′-	UGGGUCGUAGGAAUGUACGAU – 5′	
amiR-*ap1*A^P	Monomer (0)	*AP1* mRNA	770-790	AUCCAGCAUCCUUACAUGCUC	−43.14
				||||||||||||||||||||	
		amiR-*ap1*A^P	3′-	UAGGUCGUAGGAAUGUACGAG – 5′	
amiR-*ap1*AA	Dimer (1.5)	Homodimeric amiR-*ap1*A			
amiR-*ap1*AAA	Trimer (1.5)	Homodimeric amiR-*ap1*A			
amiR-*ap1*B	Monomer (3)	*AP1* mRNA	725-745	CAAGGCCACAAUAUGCCUCCC	−35.03
				| |||| |||||||||||	
		amiR-*ap1*B	3′-	GCUCCGCUGUUAUACGGAGGU – 5′	
amiR-*cal*A	Monomer (2)	*CAL* mRNA	337-357	GCACCUGACUCUCACGUUAAU	−35.27
				|| |||||||||||||||||	
		amiR-*cal*A	3′-	CGCGGACUGAGAGUGCAAUUU – 5′	
amiR-*ap1*A*cal*A	Dimer	Heterodimeric amiRNA precursor composed of amiR-*ap*1A and amiR-*cal*A			
amiR-*ap1*A^P*cal*A	Dimer	Heterodimeric amiRNA precursor composed of amiR-*ap*1A^P & amiR-*cal*A			

[a] AA or AAA denotes an amiRNA construct containing two or three hairpin repeats in tandem

Table 2 Efficiency of different forms of amiR-*ap1*

Transgenic line	No. of T1[a]	No. of T1 with WT[b] phenotype (%)	No. of T1 with mutant phenotype		Efficiency (%)
			Weak (%)	Strong (%)	
amiR-*ap1*A	41	24 (58.5)	9 (22)	8 (19.5)	41.5
amiR-*ap1*AAA	37	8 (21.6)	20 (54.1)	9 (24.3)	78.4
amiR-*ap1*A^P	33	1 (3)	13 (39.4)	19 (57.6)	97
amiR-*ap1*B	20	20 (100)	0	0	0

[a] Number of independent T1 transformants analyzed

[b] Wild-type plants

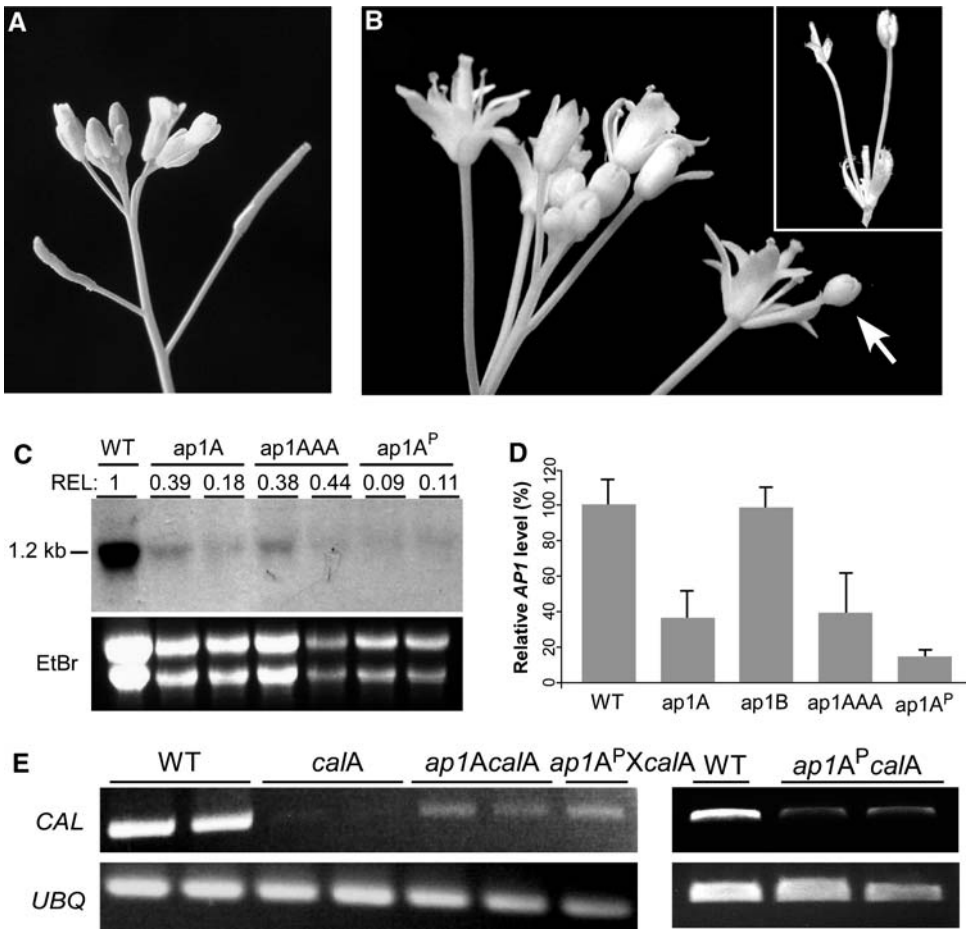

Fig. 2 Improved gene silencing by modified amiRNAs. Floral mutant phenotypes and *AP1* mRNA expression levels were analyzed and compared. **a** Inflorescence of wild-type *Arabidopsis* Col-0. **b** Representative strong mutant flowers taken from an amiR-*ap1*AAA T1 plant. *Arrow* and the inset show abnormal flower production from the base of leaf-like organ. **c** RNA blot sowing the detection of ~1.2 kb *AP1*mRNA hybridized with ^{32}P-labeled *AP1*-specific cDNA probe (*upper panel*). Loading of total RNAs is shown in EtBr-stained gel (*bottom panel*). Relative *AP1* expression level (*REL*) in different genetic backgrounds was estimated in a densitometric analysis by normalizing the hybridization band intensity against the total RNA loading amount. Two independent T1 lines from each group of transgenic plants were analyzed. **d** Relative *AP1* mRNA expression levels in wild-type (*WT*) and different transgenic lines determined by semi-quantitative RT-PCR. Each error bar represents the standard deviation of six densitometrically quantified DNA bands detected in EtBr-stained agarose gels. Band densities were normalized against the *UBIQUITIN* level. **e** Detection of *CAL* mRNA levels in transgenic plants by semi-quantitative RT-PCR. RT-PCR for *UBQ* is shown as loading control

also exhibited higher occurrence of mutant flowers within individual plants compared with the transgenic plants that express monomeric or trimeric amiR-*ap1*A constructs (Table 2). More than half of these plants exhibited strong *ap1* mutant alleles, producing secondary flowers at the base of leaf-like organs of primary flowers (Fig. 2b). Moreover, RT-PCR analysis revealed that the level of *AP1* mRNA expression was reduced by ~85% in amiR-*ap1*A^P plants (Fig. 2d), indicating a high potency of amiR-*ap1*A^P toward *AP1* mRNA down-regulation. These results suggested that incorporation of mismatches between the amiRNA and its target site might not be necessary for efficiently inducing

amiRNA-based gene silencing, although it could vary depending on target genes.

A simultaneous gene silencing by using multimeric amiRNAs targeting *AP1* and *CAL*

To further examine whether the effect of *AP1* gene silencing brought about by the amiR-*ap1*A^{P} was significantly more effective than amiR-*ap1*A, we introduced heterodimeric forms of amiRNAs targeting both *AP1* and *CAL* genes, amiR-*ap1*A*cal*A and amiR-*ap1*A^{P}*cal*A. *CAL* plays partially redundant function with *AP1*. It was shown that mutations in *CAL* gene alone did not manifest floral organ defects, while a combination between *cal* and strong *ap1* alleles resulted in formation of indeterminate inflorescence meristems that resembled the cauliflower head (Bowman et al. 1993; Kempin et al. 1995). We reasoned that if amiR-*ap1*A^{P}*cal*A but not amiR-*ap1*A*cal*A induces cauliflower-like phenotype, this would strongly support that amiR-*ap1*A^{P} was more potent than the unmodified form. First, we produced transgenic plants that express amiR-*cal*A (Table 1) and confirmed by RT-PCR that this amiRNA was functional in downregulating *CAL* mRNA (Fig. 2e). Consistent with the published works, down-regulation of *CAL* did not cause any floral defects in amiR-*cal*A plants (Table 3). We then produced heterodimeric amiRNAs consisted of amiR-*ap1*A*cal*A or amiR-*ap1*A^{P}*cal*A and compared phenotypes of the transgenic plants that express these amiRNAs. Both amiRNAs were overall highly efficient (94%) in producing T1 plants with floral phenotypes (Table 3). However, whereas all the amiR-*ap1*A*cal*A T1 plants resembled only weak *ap1 cal* alleles, 33% amiR-*ap1*A^{P}*cal*A T1 plants revealed an *ap1 cal* null phenotype reminiscent of cauliflower mutant phenotype (Fig. 3b; Table 3).

Although unlikely, there was a possibility that the cauliflower-like phenotype revealed by amiR-*ap1*A^{P}*cal*A plants was due to the difference in *CAL* mRNA expression level. But this possibility could be ruled out as the levels of *CAL* mRNA expression in both transgenic groups were similarly reduced by ~80% (see Fig. 2e). On the other hand, the reduction rate of *AP1* mRNA expression level was slightly higher in amiR-*ap1*A^{P}*cal*A plants than in amiR-*ap1*A*cal*A plants (Fig. 3d). Consistent results were observed when an F1 population produced by crossing the amiR-*ap1*A^{P} T1 plants with amiR-*cal*A T1 plants was phenotypically analyzed. One quarter of these plants were genetically wild-type, indicating that both the parental T1 lines were hemizygous. Among the F1 plants showing strong morphological phenotypes, ~30% plants exhibited near null phenotype with cauliflower-like indeterminate meristems (Table 3; Fig. 3c). These results support that the cauliflower-like phenotype revealed by amiR-*ap1*A^{P}*cal*A plants was likely due to its relatively higher effectiveness of *AP1* silencing by the modified amiR-*ap1*A^{P}. To demonstrate that the multimeric amiR-*ap1*A*cal*A was functional in cleaving *AP1* and *CAL* mRNA transcripts, we then performed 5′RACE-PCR and mapped the amiRNA-guided target cleavage sites. RACE-PCR resulted in amplifying discrete fragments expected for both *AP1* and *CAL* cleavage products from amiR-*ap1*A*cal*A transgenic plants (data not shown), and the sequencing of the PCR clones conformed to the predicted cleavage sites (Fig. 3e). Collectively, these data demonstrated that a more effective RNAi could be achieved through modifying the existing amiRNA design and independent genes can be efficiently downregulated by expressing heteromeric tandem amiRNAs.

AP1 methylation status in amiR-*ap1*A, amiR-*ap1*AAA, and amiR-*ap1*A^{P} plants

To gain molecular insight into the differential gene silencing efficiency induced by altered forms of amiRNAs

Table 3 Gene silencing effect of heterodimeric amiRNAs

Transgenic line	No. of independent transformants[a]	No. of plants with mutant phenotypes			Efficiency (%)	Effectiveness[c] (%)
		None[b] (%)	Weak (%)	Strong (%)		
amiR-*cal*A	16	NA			NA	NA
amiR-*ap1*A*calA*	17	1 (6)	16 (94)	0	94	0
amiR-*ap1*A^{P}*calA*	15	1 (6.7)	9 (60)	5[d] (33.3)	93.3	100
amiR-*ap1*A^{P}/amiR-*calA*	31[e]	10 (32)	9 (29)	12[f] (39)	NA	NA

NA not applicable

[a] T1 or F1 plants were analyzed

[b] Plants showing wild-type phenotype

[c] Percentage of plants with null mutant phenotype showing indeterminate meristems among plants scored for strong phenotype

[d] All 5 plants with strong *ap1 cal* phenotype produced indeterminate meristems

[e] Among segregating F1 progenies, only bar-resistant plants were scored

[f] Four out of twelve plants with strong *ap1 cal* phenotype produced indeterminate meristems

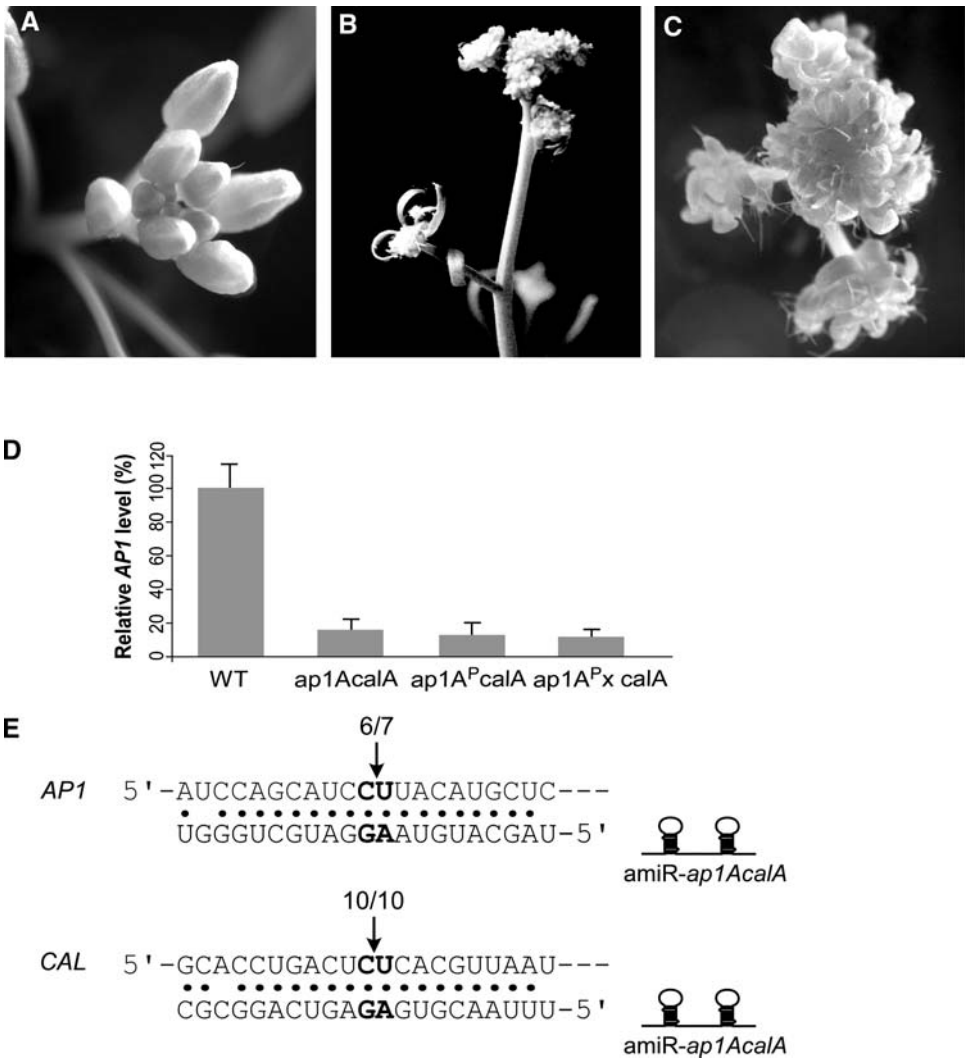

Fig. 3 Efficiency of heterodimeric amiRNAs. Floral mutant phenotypes and *AP1* mRNA expression levels in amiR-*ap1*A*cal*A and -*ap1*A^{P}*cal*A plants were analyzed and compared. **a** Inflorescence of wild-type *Arabidopsis*. **b** A representative cauliflower-like phenotype exhibited by amiR-*ap1*A^{P}*cal*A T1 plants. **c** Cauliflower-like phenotype observed in F1 plants as control that are produced by crossing amiR-*ap1*A^{P} and amiR-*cal*A T1 plants. **d** Relative *AP1* mRNA expression levels in wild-type (*WT*) and different transgenic lines determined by semi-quantitative RT-PCR. *Error bars* represent the standard deviation of four quantified DNA bands. **e** Mapping of amiR-*ap1*A*cal*A-guided *AP1* and *CAL* transcript cleavage sites by 5′ RACE-PCR. *Numbers* above *arrows* indicate the number of clones ending at that site and the total number of clones

tested in our study, we assessed whether it was correlated with either the level of amiRNA accumulation or the methylation status of target genomic loci. We first investigated whether differential methylation of the *AP1* gene correlated with the extent of the gene silencing effect. It was reported that small silencing RNAs, whether having perfect or imperfect sequence complementarity to the targets, could induce gene silencing by modulating chromatin modification through DNA methylation (Bao et al. 2004; Vaucheret 2006). Since amiR-*ap1*A^{P} is designed to have perfect base-paring with its respective *AP1* target site, we suspected that the effectiveness associated with this amiRNA construct is correlated with the DNA methylation status. This experiment was performed by choosing two methylation-sensitive *Hae*III sites within the *AP1* gene and testing whether the amplification of DNA fragments spanning these sites, PCR1 or PCR2, was affected by pre-incubation with *Hae*III (Fig. 4). If these *Hae*III sites were methylated, the PCR products would be amplified regardless of the enzyme treatment because the DNA would not be digested by the enzyme. However, if the *Hae*III sites were not methylated, enzyme treatment would prevent amplification of the PCR products.

The *Hae*III site within the PCR1 but not PCR2 region was found not methylated and thus only a minimal amount of PCR1 fragment was amplified from the wild-type genomic DNA pretreated with *Hae*III compared to the untreated sample (Fig. 4). In contrast, amplification of the PCR1 fragment was insensitive to *Hae*III treatment from the DNA extracted from silencing lines, suggesting that methylation of *AP1* gene at this site was promoted in the transgenic plants. However, all the transgenic plant samples tested showed a similar level of amplification of the PCR1 fragment upon *Hae*III treatment. Based on this result, it was unlikely that the differential effectiveness of gene silencing caused by altered amiRNAs is directly linked to this methylation event.

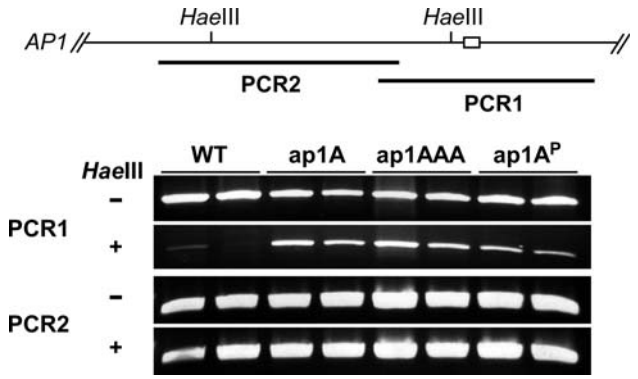

Fig. 4 Methylation status of *AP1* locus measured by PCR coupled with methylation-sensitive restriction enzyme *Hae*III. *Boxed* region indicates the amiRNA target site. Genomic DNAs, extracted from two independent plants from each group, were used to ampify PCR1 and PCR2 fragments spanning *Hae*III sites following the incubation in the presence or absence of the enzyme. PCR products were fractionated in agarose gels and stained with EtBr

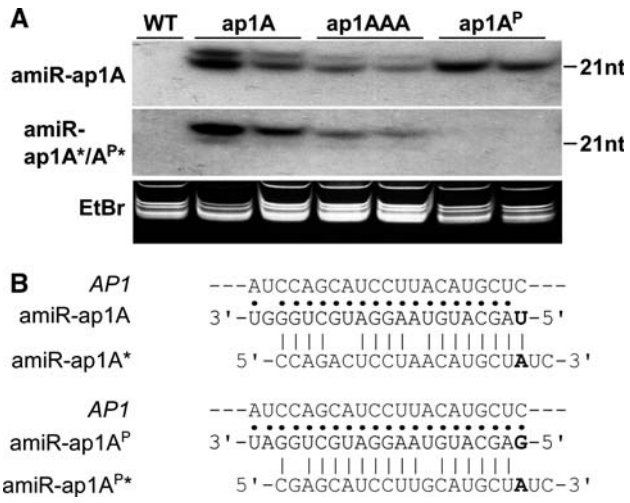

Fig. 5 Differential accumulation of small amiRNAs. **a** Expression level of small amiRNAs. The RNA blot hybridized with ^{32}P-labeled oligo nucleotide probes shows the detection of processed amiR-*ap1*A (*top panel*) or amiR-*ap1*A*/A^{P}* (*middle panel*). Loading of total RNAs is shown in EtBr-stained acrylamide gel (*bottom panel*). The size of small RNAs was approximated by a 21-nt DNA oligomer run simultaneously in the gel. **b** Sequences of the *AP1* target and amiRNA duplexes are shown to visualize relative complementarities between the target and amiRNA and between amiRNA and amiRNA* strands

Differential processing of amiR-*ap1*A, amiR-*ap1*AAA, and amiR-*ap1*A^{P}

Next, we analyzed the expression level of *AP1*-specific amiRNAs in amiR-*ap1*A, amiR-*ap1*AAA, and amiR-*ap1*A^{P} plants. Total RNAs were extracted from these transgenic lines as well as wild-type *Arabidopsis* as a control and separated in denaturing 15% polyacrylamide gels. The RNAs were then electroblotted onto a positively-charged nylon membrane followed by blot hybridization with radio-labeled oligonucleotide probes specific to amiR-*ap1*A or amiR-*ap1*A*/A^{P}*. As expected, amiR-*ap1*A was detected in all independent transgenic lines tested but not in wild-type plants (Fig. 5a). In all three transgenic groups, a major 21 nucleotide (nt)-long amiR-*ap1*A band was detected. However, the expression level of different amiRNAs did not correlate with the *AP1* mRNA reduction rate or strength of the morphological phenotypes. Expression level of 21 nt amiRNAs was similar in amiR-*ap1*A and amiR-*ap1*A^{P} plants but lower in amiR-*ap1*AAA plants. Detection of a lower level of amiRNA accumulation in amiR-*ap1*AAA plants was unexpected as we anticipated that multimeric amiRNAs could increase the accumulation of amiRNAs as observed in animal system (Sun et al. 2006).

Intriguingly, an additional band slightly longer than 21mer was present in amiR-*ap1*A and amiR-*ap1*AAA plants but not in amiR-*ap1*A^{P} plants. In amiR-*ap1*A and amiR-*ap1*AAA plants, accumulation of amiR-*ap1*A* strand corresponding to 22–24 nt was detected at different intensities. This band was similar in size to the secondary amiR-*ap1*A strand detected in the amiR-*ap1*A and amiR-*ap1*AAA plants. Similar results were observed in transgenic plants that express *ap1*A*cal*A and *ap1*A^{P}*cal*A (data not shown). We concluded that the level of amiRNA expression in each transgenic plant group was sufficient to induce gene silencing, but a correlation between the expression level of different amiRNAs and their effectiveness could not be drawn. Rather, it appeared that an inverse relationship between the accumulation of secondary (22-24 nt-long) amiRNA or amiRNA* strand and the gene silencing efficiency might exist.

Alternatively, more efficient biogenesis of mature amiRNA and fast degradation of amiRNA* strand in amiR-*ap1*A^{P} plants may explain the potency of amiR-*ap1*A^{P}. The predominant accumulation of 21 nt amiR-*ap1*A^{P} in contrast to an undetectable level of amiR-*ap1*A^{P}* (Fig. 5a) supports this notion. When amiR-*ap1*A^{P} was designed, U-to-G substitution at the 5′ nucleotide position 1 of the amiRNA strand had to be made to perfectly complement the *AP1* target sequence (Fig. 5b). Concomitantly, to provide the mature amiR-*ap1*A^{P} with 5′ terminal instability and asymmetry (Khvorova et al. 2003; Schwab et al. 2006), a G–A mismatch between amiRNA and amiRNA* strands was introduced. This alteration in amiRNA duplex structure may have aided Dicer to predominantly produce the 21 nt amiR-*ap1*A^{P} duplex and facilitated Argonaut to preferentially load the amiRNA strand and degenerate the amiR-*ap1*A^{P}* strand, whereas U:A pairing at the 5′ terminus allowed in the amiR-*ap1*A duplex was not as effective.

Discussion

In this study, we showed that altered forms of amiRNAs with simple modifications such as those containing no

mismatches to the respective target genes and 5′ mismatch within the mature amiRNA duplex or multimeric forms were highly effective in degrading target mRNAs and mimicking null mutant phenotypes. One advantage of allowing perfect complementarity between amiRNA and its target sequence is that this may confer higher target-specificity in gene silencing. Multimeric amiRNAs can be especially useful in simultaneously knocking down redundant genes when designing a single amiRNA that targets multiple members is not feasible. In our study, we produced heterodimeric amiRNAs by simply fusing full-length amiRNA precursors in tandem. This approach could be further optimized by testing different lengths or identifying minimal sequence requirements between amiRNAs or amiRNA precursors if simultaneous gene silencing of several genes is desired.

Recently, a natural tandem miRNA expressed endogenously as one transcriptional unit was found in maize (Chuck et al. 2007). Maize mutant *Corngrass1* (*Cg1*) was shown to overexpress two tandem miRNAs, miR156b/c, the phenotype of which was mimicked by ectopic expression of the miRNA under a constitutive promoter. This tandem miRNA is conserved among cereals but not found in dicots (Wang et al. 2007). However, it is likely that dicots also have a molecular mechanism to process tandem miRNAs to mature functional forms. Niu et al. (2006) showed that expression of dimeric amiRNA precursors that target two different viruses conferred resistance to both viruses in transgenic *Arabidopsis* plants. Our study also provides experimental support that a simultaneous knock-down of endogenous genes in *Arabidopsis* can be efficiently achieved. It was recently demonstrated that miRNA tandem repeats were more effective than a single-hairpin in animal systems (Sun et al. 2006). These data collectively suggest that a common mechanism by which multimeric amiRNAs or naturally occurring polycistronic miRNAs (Tanzer and Stadler 2004) are processed exists both in animal and plant systems.

It is notable that near knock-out mutant phenotypes were observed with the amiR-*ap1*A^{P}, which is modified to have perfect complementarity with the target sequence. The potency of amiR-*ap1*A^{P} was also demonstrated in transgenic plants that express heterodimeric amiR-*ap1*A^{P}*cal*A (see Fig 3; Table 3). In these plants, the severity of morphological phenotypes appeared to accompany respective reductions in *AP1* mRNA level, exhibiting the highest reduction in amiR-*ap1*A^{P} plants followed by amiR-*ap1*AAA and amiR-*ap1*A plants. Intriguingly, secondary amiRNA and amiRNA* bands detected in the transgenic plants that express amiRNA precursors, amiR-*ap1*A and -*ap1*AAA were absent in the amiR-*ap1*A^{P} plants (see Fig. 5). These larger amiRNA and amiRNA* strands might have been processed to a stable duplex and could be either simply non-functional byproducts or somewhat competitive to the 21 nt amiRNAs. Apparent differences in mature miRNA processing in these plants implies that either the sequence complementarity between the amiRNAs and the target mRNA or, more likely, the structure of amiRNA duplex may have influenced over their processing. It is possible that an efficient biogenesis of mature amiR-*ap1*A^{P} duplex coupled with fast discharge/degradation of amiR-*ap1*A^{P}* strand by Argonaut could account for its strong target gene silencing.

What makes amiR-*ap1*A^{P} so potent? Since the amiR-*ap1*A and amiR-*ap1*A^{P} had differences not only in target complementarity but also in the structure of amiRNA duplex, it is difficult to pinpoint which change had the bigger role. It is conceivable that the higher sequence specificity conferred by amiR-*ap1*A^{P} may have been more effective or favorable in targeting *AP1* for degradation, as we had initially anticipated based on the lower binding energy. Or, in terms of target degradation, perhaps perfect sequence complememtarity does not interfere with RISC activity. Consistently, we and others have observed that various amiRNAs perfectly complementing their target sequences were functionally efficient (W. Park, J.-Y. Lee, unpublished data and personal communication with M. Aukerman at DuPont; Niu et al. 2006). Conferring the 5′ instability and having U at position 1 of amiRNAs is considered an important factor for designing effective amiRNAs (Ossowski et al. 2008), but the G–A mismatch is generally not favored in designing amiRNAs in plant systems. In animal systems, however, the 5′ G–A mismatch or U:G wobble was shown to be highly potent in generating functionally asymmetric siRNA duplex whose structures facilitate one strand to be loaded into the RISC but the other to be degraded (Schwab et al. 2006). This mechanism has not yet been demonstrated in plant systems but helps explain our observation that the accumulation of amiR-*ap1*A^{P}* strand was undetectable. Future investigation into this possibility would prove insightful in elucidating the underlying molecular mechanism as well as further improving the amiRNA design.

Another possibility underlying observed potency of amiR-*ap1*A^{P} could be that transitive siRNAs might have been generated due to perfect complementary between the amiRNA and *AP1* target gene. Our observation that the RNAi lines revealed expected *ap1* or *ap1 cal* phenotypes without obvious unrelated defects negates potential non-specificity associated with amiR-*ap1*A^{P}. However, it is conceivable that the perfect complementarity between amiR-*ap1*A^{P} and *AP1* employed in our study may have compromised the highly specific nature of miRNAs, and additional tests will be necessary to determine whether amiR-*ap1*A^{P} triggered the production of transitive siRNA. It was previously demonstrated that miRNAs with perfect

complementarity to their exogenous targets can trigger transitive RNA silencing (Parizotto et al. 2004). On the other hand, amiRNAs designed to target viral genes with perfect complementarity has shown high specificity toward the viral genes without affecting endogenous genes (Niu et al. 2006). These studies and our results suggest that the amiRNA design incorporating perfect complementary to a target gene could be advantageous in increasing gene silencing efficiency as well as simplifying the design when used with caution.

It is estimated that the overall success rate of amiRNA-based gene silencing is close to 75% (Ossowski et al. 2008). Although certain target genes may be recalcitrant to RNAi, it suggests that the amiRNA design is not maximally optimized. A systematic manipulation of amiRNA structure and sequence may prove useful to further enhance the effectiveness of amiRNA in plants and to elucidate underlying mechanisms. Our study presented here provides experimental evidence that designing amiRNAs with perfect complementarity to the target genes in combination with strong 5′ instability introduced by G–A mismatch would be a new effective approach.

Acknowledgments We owe thanks to M. Aukerman and B.-C. Yoo for helpful discussions and comments on the manuscript and H. Frick and R. Sager for careful proofreading. We also thank D. Weigel for providing pRS300 plasmid vector. This research was supported by the National Institutes of Health COBRE (P20 RR15588) and DuPont Young Professorship awarded to J.-Y. L.

References

Alvarez JP, Pekker I, Goldshmidt A, Blum E, Amsellem Z, Eshed Y (2006) Endogenous and synthetic microRNAs stimulate simultaneous, efficient, and localized regulation of multiple targets in diverse species. Plant Cell 18:1134–1151

Aukerman MJ, Sakai H (2003) Regulation of flowering time and floral organ identity by a MicroRNA and its APETALA2-like target genes. Plant Cell 15:2730–2741

Bao N, Lye KW, Barton MK (2004) MicroRNA binding sites in Arabidopsis class III HD-ZIP mRNAs are required for methylation of the template chromosome. Dev Cell 7:653–662

Bartel DP (2004) MicroRNAs: genomics, biogenesis, mechanism, and function. Cell 116:281–297

Baulcombe D (2004) RNA silencing in plants. Nature 431:356–363

Bowman JL, Alvarez J, Weigel D, Meyerowitz EM, Smyth DR (1993) Control of flower development in *Arabidopsis thaliana* by APETALA1 and interacting genes. Development 119:721–743

Brodersen P, Sakvarelidze-Achard L, Bruun-Rasmussen M, Dunoyer P, Yamamoto YY, Sieburth L, Voinnet O (2008) Widespread translational inhibition by plant miRNAs and siRNAs. Science 320:1185–1190

Brodersen P, Voinnet O (2006) The diversity of RNA silencing pathways in plants. Trends Genet 22:268–280

Chen X (2004) A MicroRNA as a translational repressor of APETALA2 in *Arabidopsis* flower development. Science 303:2022–2025

Chuang CF, Meyerowitz EM (2000) Specific and heritable genetic interference by double-stranded RNA in Arabidopsis thaliana. Proc Natl Acad Sci USA 97:4985–4990

Chuck G, Cigan AM, Saeteurn K, Hake S (2007) The heterochronic maize mutant Corngrass1 results from overexpression of a tandem microRNA. Nat Genet 39:544–549

Filipowicz W, Bhattacharyya SN, Sonenberg N (2008) Mechanisms of post-transcriptional regulation by microRNAs: are the answers in sight? Nat Rev Genet 9:102–114

Kempin SA, Savidge B, Yanofsky MF (1995) Molecular basis of the cauliflower phenotype in *Arabidopsis*. Science 267:522–525

Khvorova A, Reynolds A, Jayasena SD (2003) Functional siRNAs and miRNAs exhibit strand bias. Cell 115:209–216

Liu Y, Schiff M, Marathe R, Dinesh-Kumar SP (2002) Tobacco Rar1, EDS1 and NPR1/NIM1 like genes are required for N-mediated resistance to tobacco mosaic virus. Plant J 30:415–429

Lu R, Martin-Hernandez AM, Peart JR, Malcuit I, Baulcombe DC (2003) Virus-induced gene silencing in plants. Methods 30:296–303

Mandel MA, Gustafson-Brown C, Savidge B, Yanofsky MF (1992) Molecular characterization of the *Arabidopsis* floral homeotic gene APETALA1. Nature 360:273–277

Niu QW, Lin SS, Reyes JL, Chen KC, Wu HW, Yeh SD, Chua NH (2006) Expression of artificial microRNAs in transgenic *Arabidopsis thaliana* confers virus resistance. Nat Biotechnol 24:1420–1428

Onodera Y, Haag JR, Ream T, Nunes PC, Pontes O, Pikaard CS (2005) Plant nuclear RNA polymerase IV mediates siRNA and DNA methylation-dependent heterochromatin formation. Cell 120:613–622

Ossowski S, Schwab R, Weigel D (2008) Gene silencing in plants using artificial microRNAs and other small RNAs. Plant J 53:674–690

Palatnik JF, Allen E, Wu X, Schommer C, Schwab R, Carrington JC, Weigel D (2003) Control of leaf morphogenesis by microRNAs. Nature 425:257–263

Palatnik JF, Wollmann H, Schommer C, Schwab R, Boisbouvier J, Rodriguez R, Warthmann N, Allen E, Dezulian T, Huson D, Carrington JC, Weigel D (2007) Sequence and expression differences underlie functional specialization of arabidopsis microRNAs miR159 and miR319. Dev Cell 13:115–125

Parizotto EA, Dunoyer P, Rahm N, Himber C, Voinnet O (2004) In vivo investigation of the transcription, processing, endonucleolytic activity, and functional relevance of the spatial distribution of a plant miRNA. Genes Dev 18:2237–2242

Park W, Li J, Song R, Messing J, Chen X (2002) CARPEL FACTORY, a Dicer homolog, and HEN1, a novel protein, act in microRNA metabolism in Arabidopsis thaliana. Curr Biol 12:1484–1495

Schwab R, Ossowski S, Riester M, Warthmann N, Weigel D (2006) Highly specific gene silencing by artificial microRNAs in *Arabidopsis*. Plant Cell 18:1121–1133

Sun D, Melegari M, Sridhar S, Rogler CE, Zhu L (2006) Multi-miRNA hairpin method that improves gene knockdown efficiency and provides linked multi-gene knockdown. Biotechniques 41:59–63

Tanzer A, Stadler PF (2004) Molecular evolution of a microRNA cluster. J Mol Biol 339:327–335

Vaucheret H (2006) Post-transcriptional small RNA pathways in plants: mechanisms and regulations. Genes Dev 20:759–771

Wang S, Zhu QH, Guo X, Gui Y, Bao J, Helliwell C, Fan L (2007) Molecular evolution and selection of a gene encoding two tandem microRNAs in rice. FEBS Lett 581:4789–4793

Warthmann N, Chen H, Ossowski S, Weigel D, Herve P (2008) Highly specific gene silencing by artificial miRNAs in rice. PLoS ONE 3:e1829

Watson JM, Fusaro AF, Wang M, Waterhouse PM (2005) RNA silencing platforms in plants. FEBS Lett 579:5982–5987

Wesley SV, Helliwell CA, Smith NA, Wang MB, Rouse DT, Liu Q, Gooding PS, Singh SP, Abbott D, Stoutjesdijk PA, Robinson SP, Gleave AP, Green AG, Waterhouse PM (2001) Construct design for efficient, effective and high-throughput gene silencing in plants. Plant J 27:581–590